RSC Advances

ROYAL SOCIETY OF CHEMISTRY

www.rsc.org/advances

Preparation of Poly(methyl methacrylate)/Polystyrene/Poly(acrylonitrile-*co*-butadiene) Tri-layer Core-Shell Nanoparticles and their Postpolymerization Modification via Catalytic Latex Hydrogenation

Hui Wang, Lijuan Yang, Garry L. Rempel*

Department of Chemical Engineering, University of Waterloo, 200 University Ave. West, Waterloo, Ontario, N2L 3G1, Canada

*Corresponding author: Garry L. Rempel, grempel@uwaterloo.ca; Tel.: +1 519 8884567 ext. 32702. Fax: +1 519 7464979.

Abstract

Poly(methyl methacrylate)/polystyrene/poly(acrylonitrile-*co*-butadiene) (PMMA/PS/NBR) tri-layer core-shell elastomeric nanoparticles were synthesized using a facile and robust one-pot semibatch emulsion polymerization technique which allows for scale-up for industrial production. The prepared core-shell polymer nanoparticles consist of a PMMA core, PS secondary layer, and diene-containing NBR outer shell. These nanoparticles were subsequently chemically modified via a "green" postpolymerization process, i.e., catalytic latex hydrogenation without assistance of any organic solvent. As the hydrogenated product, PMMA/PS/HNBR (hydrogenated NBR) tri-layer core-shell nanoparticles were obtained. The rate of hydrogenation was considerably fast and a high degree of hydrogenation was achieved. Meanwhile no crosslinking was observed for the polymers after the hydrogenation process. This study is expected to extend the research relating to the synthesis of polymer nanoparticles with complex architecture and "green" chemical modification of unsaturated polymers in the aqueous phase.

Keywords: Core-shell polymers; Semibatch emulsion polymerization; Latex hydrogenation; Catalysis; High performance rubber.

Introduction

Recent years have seen considerable progress in the preparation methods, modification, functions, and applications of core-shell structured polymer nanoparticles.[1-3] The interest in such nanomaterials is a result that the core-shell nanostructures can render the polymers synergically outstanding physiochemical properties and tunable surface functionalities with molecular and supermolecular structures over their single-component counterparts when the core/shell heterogeneous polymer domains are optimally designed.[4-7]

Core-shell polymer nanoparticles can be divided into two categories depending on the relative hardness of the core and shell polymer domains. On the one hand, the physical composition comprised of a soft rubber core and a hard shell can provide corresponding polymers with enhanced strength and tough properties.[8,9] The core or shell can be crosslinked depending on the requirements for specific applications. The rubber core is mostly made of a low glass transition temperature (T_g) polymer while the hard shell is usually prepared from a relatively high T_g polymer. The glassy shell can be designed to increase the chemical reactivity with the polymer matrix. This type of core-shell nanoparticles are usually synthesized to act as impact modifiers due to the fact that the rubbery core provides resistance to impact especially at low temperature, whereas the hard shell not only provides rigidity and compatibility to the polymer matrix but also keeps the particles desired shape and dispersibility.[10,11] On the other hand, core-shell polymer nanoparticles can be fabricated by a stiff core and a soft shell, in which the stiff core is responsible for the stability of the particles while the flexible shell is required for the film formation after casting on surfaces.[12] These types of structured nanoparticles are commonly used as additives, coatings, paints, and binders with a high block resistance and low minimum film-forming temperature (MFFT).[13,14] Their excellent film-forming properties however are difficult

to be achieve by physical blending of two or more different polymer components.[15,16] With respect to our work, the core-shell nanoparticles we proposed to synthesize are of the second type of particles, which are constituted by a poly(methyl methacrylate)/polystyrene (PMMA/PS) stiff core-shell and a soft shell of poly(acrylonitrile-*co*-butadiene) (NBR) rubber. A PMMA/PS combination is designed to endow the improvements in the physicochemical properties by taking advantage of the unique properties of PMMA and PS, which for example can be used as a reinforcing filler by adjusting the ratio of PMMA and PS. The outer shell NBR or HNBR (the subsequent hydrogenated product of NBR) provide important rubber products and especially HNBR as it is used as a high performance speciality rubber. NBR and HNBR based elastomers are playing an increasingly important role in a diverse range of industrial applications such as automobile components and oil drilling devices.

Core-shell polymers are generally prepared by two methods. The first one is a multistage seeded tandem polymerization particularly carried out in a (micro)emulsion media.[17-21] The second one is the self-assembly of the polymerization-induced block copolymer aggregates, which is performed preferably in the polymer solution.[22-24] These two methods are most well-known and widely used to prepare the core-shell polymers, which however does not exclude the utilization of other techniques including a hetero-coagulation strategy,[25] precipitation polymerization,[26] and distillation precipitation polymerization.[27] Among these various techniques, multistage seeded emulsion polymerization has been practiced frequently. In this method, polymerization of the shell forming monomer is performed on the surface of the core seeded particles, thus, producing core-shell microspheres. The seeded monomers of the first stages can either polymerize beforehand in a separate step (so-called “dead” or inactive seeding) or *in situ* during the emulsion polymerization (so-called “live” or active seeding). The addition of

monomers at the first stage and the successive stages can be in a semibatch addition manner (monomer starved feeding) or a batch swelling manner depending on the specific circumstances.

In our previous studies, the uniform spherical NBR nanoparticles[28] and PMMA/NBR core-shell nanoparticles (with PMMA and NBR as the core and shell respectively)[29] have been synthesized via a GS 12-3-12 emulsified semibatch emulsion polymerization. GS 12-3-12 is the denotation of Gemini surfactant trimethylene-1,3-bis(dodecyldimethylammonium bromide) (molar mass 628.69 g/mol). A Gemini surfactant is an amphiphile made up of two conventional surfactant molecules chemically bonded together by a spacer moiety, which features a lower critical micelle concentration (e.g., CMC = 1 mM or ~0.63 g/L for GS 12-3-12) and greatly increased interfacial activity compared to conventional surfactants.[30,31]

As a process-development oriented research and for technical interest, herein we describe the preparation of PMMA/PS/NBR tri-layer core-shell nanoparticles by seeded emulsion polymerization using a three-stage *in situ* semibatch mode by means of which allows scale-up for industrial production of latex particles. In this operational process, all of the monomers including the core monomer MMA were all sequentially charged into the reaction system via a dropwise manner (where monomer starved was produced) in an one-pot semibatch reactor. A short term three-stage semibatch emulsion polymerization was used to describe the above process for the facilitation of the following discussions. The prepared unsaturated PMMA/PS/NBR nanoparticles were then directly hydrogenated in latex form in the presence of Wilkinson's catalyst $RhCl(P(C_6H_5)_3)_3$ to prepare PMMA/PS/HNBR nanoparticles. Latex hydrogenation is a postpolymerization "green" process to directly hydrogenate the unsaturated polymer particles in a stable dispersion (emulsion) preferably in an aqueous medium. The detailed description and fundamental chemistry related to the latex hydrogenation can be found in preceding articles.[32,33]

Results and discussion

Semibatch emulsion polymerization is a unique process for manufacturing fine polymer nanoparticles. By controlling the monomer feeding rate, the polymer chain growing radicals will consume the monomer molecules faster than the rate of monomer molecules added into the reaction system, creating a monomer "starved" condition which is maintained until the end of the polymerization. Therefore, the monomer molecules are considered to be delivered to the reaction locus from an external reservoir through a physical means rather than from the interior of nanodroplets (e.g., microemulsion mechanism). The monomer-starved semibatch microemulsion polymerization provides a practical way to enhance particle formation and thus to produce nanolatex. It has been recently shown that this process can produce a large number of small particles.[28,29,34]

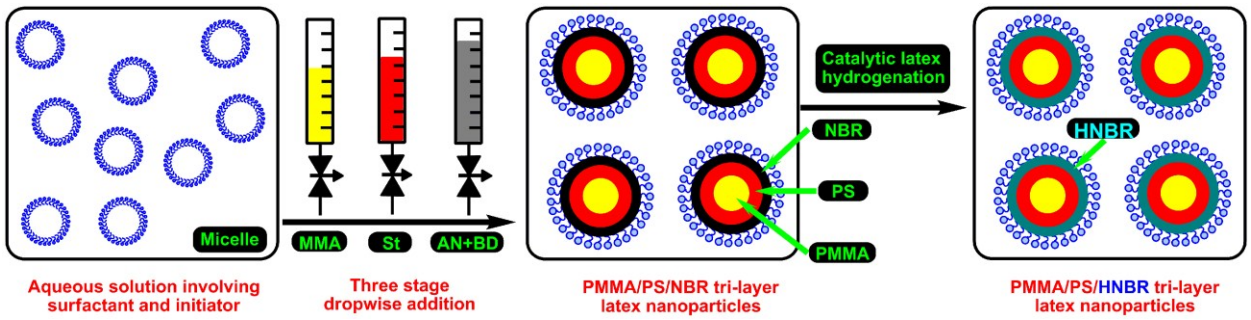

Figure 1. Schematic diagram illustrating the synthesis and catalytic latex hydrogenation of diene-contained PMMA/PS/NBR tri-layer core-shell nanoparticles.

Figure 1 schematically represents the preparation of PMMA/PS/NBR and PMMA/PS/HNBR tri-layer core-shell nanoparticles. In the reaction process, the PMMA/PS/NBR core-shell nanoparticles are reproducibly prepared by a one-pot three-stage semibatch emulsion polymerization. The first stage monomer MMA, second stage monomer PS, and third stage

monomers acrylonitrile (AN) and 1,3-butadiene (BD) (homogenous mixture) were all sequentially charged into one semibatch reaction system under monomer-starved conditions. The PMMA/PS/NBR latex obtained at the end of reaction was first treated using vacuum distillation to remove the residual BD and most of the unreacted acrylonitrile AN. The remaining portion of AN was eliminated by steam distillation at 70 ℃ under reduced pressure since the remaining organic chemicals such as AN in the latex may affect the catalytic activity of the catalyst. The catalytic latex hydrogenation was then carried out upon the diene-contained PMMA/PS/NBR nanoparticles using $RhCl(P(C_6H_5)_3)_3$ in the same reactor as used for the synthesis reactions. PMMA/PS/HNBR was finally obtained as the hydrogenated product. The process of this emulsion synthesis potentially provides additional particle design features such as a modification of the outer or inner surfaces by functional groups. One can also replace the NBR layer with other diene-containing rubbers which allow for subsequent catalytic hydrogenation; for example styrene butadiene rubber (SBR) and polybutadiene rubber (BR).

Table 1 Formulation recipe, reaction conditions, and principal characteristics for synthesizing PMMA, PMMA/PS core-shell, and PMMA/PS/NBR tri-layer core-shell nanoparticles

Latex label	First stage	Second stage	Third stage
Particle type	PMMA	PMMA/PS core-shell	PMMA/PS/NBR tri-layer core-shell
Temperature (℃)	70	70	45
Stirring	Parr stirred reactor	Parr stirred reactor	Parr stirred reactor
Turbine type	Four-blade impeller	Four-blade impeller	Four-blade impeller
Distance from reactor floor (mm)	15	15	15
Speed (rpm)	200	200	200
Water (g)	80	No additional water	No additional water
$(NH_4)_2S_2O_8$ (APS, g)	0.15	No additional initiator	No additional initiator
GS 12-3-12 (g)	2.5	No additional surfactant	No additional surfactant
MMA (g)	4.7	–	–
St (g)	–	9.1	–
AN and BD mixture (g)	–	–	13.7 (Homogenous mixture of AN and BD)
AN (g)	–	–	4.1
BD (g)	–	–	9.6
Monomer feed mode	Semibatch	*In situ* semibatch	*In situ* semibatch
Feed rate (g/min)	0.047	0.045	0.034
Reaction time after completion of monomer feeding (h)	1	1, including the time consumed for temperature dropping from 70 to 45 ℃	5
Conversion			
MMA (wt%)	85.6		
St(wt%)		87.2	
AN (wt%)	–	–	83.1
BD (wt%)	–	–	78.4
Bound level of nitrile in NBR shell (wt%)[a]	–	–	31.0
Solids content (wt%)[b]	4.6	12.7	21.7
Molecular weight[c]		GPC data	
M_n	6.5×10^5	7.6×10^5	6.3×10^5
M_w	1.7×10^6	2.2×10^6	1.9×10^6
PDI=M_w/M_n	2.6	2.9	3.0
Particle diameter (nm)[d]		DLS data	
D_n (nm)	20.7	38.6	51.3
D_z (nm)	24.1	45.2	62.5
Dispersity of size (D_z/D_n)	1.16	1.17	1.22

[a]Determined via FT-IR analysis and the analysis method can be found in Ref [29].
[b]The solid content (S%) of the polymer emulsion was determined by the weights of dried polymer and polymer latex.
[c]M_n and M_w were determined by GPC and reported as the number-average molecular weight and weight-average molecular weight, respectively.
[d]D_n and D_z were determined by DLS technique and reported as the number average diameter and the intensity average diameter, respectively.

Table 1 provides the principal characteristics of PMMA, PMMA/PS core-shell, and PMMA/PS/NBR tri-layer core-shell nanoparticles obtained in this semibatch process. The final latex product has a solid content of 21.7 wt% and the NBR outer layer contains 31 wt% bound level of nitrile. The D_n (number-average diameter) and D_z (intensity-average diameter) of PMMA/PS/NBR nanoparticles are 51.3 nm and 62.5 nm, respectively. The size of PMMA, PMMA/PS, and PMMA/PS/NBR nanoparticles was observed to increase appreciably after each stage of polymerization compared to the ones obtained at the previous stage of polymerization. This pronounced growth indicates that the monomers added during each stage of the reaction were polymerized over the core precursor nanoparticles. TEM imaging also confirms the formation of core-shell structures, as will be discussed later. Figure 2 shows the particle size distributions (PSD) by intensity for the PMMA, PMMA/PS, and PMMA/PS/NBR nanoparticles, respectively. It can be seen that the all of the latex nanoparticles present a monomodal and narrow distribution of particle size. The PSD can be further quantitatively evaluated by the ratio of D_z/D_n. D_z/D_n values ranging from 1.0-1.1 indicating that the particles are monodispersed while those ranging from 1.1-1.2 are near-monodispersed.[29] The dipsersity values of particle size presented in Table 1 suggest that near-monodisperse narrow distributions for PMMA and PMMA/PS nanoparticles can be achieved and PMMA/PS/NBR nanoparticles have a relativley higher dispersity of 1.22. On the other hand, high molecular weights of PMMA, PMMA/PS, and PMMA/PS/NBR are obtained, e.g., the M_w are all above 10^6. The PDIs (M_w/M_n) of these three types of polymers are found between 2 and 3, which indicates that the termination of the growing polymer chain mainly occurs by chain transfer to monomer.[35] This is consistent with the behavior of chain termination in normal microemulsion polymerization.

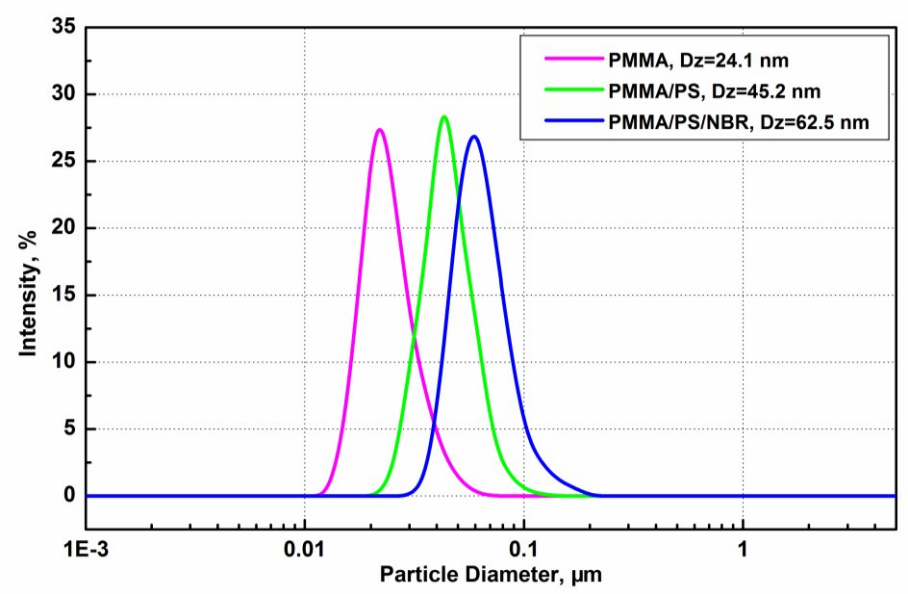

Figure 2. Particle size distributions by intensity of PMMA, PMMA/PS core-shell and PMMA/PS/NBR tri-layer core-shell nanoparticles. **Polymerization conditions**: APS = 0.15 g, Gemini Surfactant 12-3-12 = 2.5 g, MMA = 5 mL, T = 70 ℃, distilled water = 80 mL at the first stage; St = 10 mL, T = 70 ℃ at the second stage; AN = 5 mL, BD = 15 mL, T = 45 ℃ at the third stage.

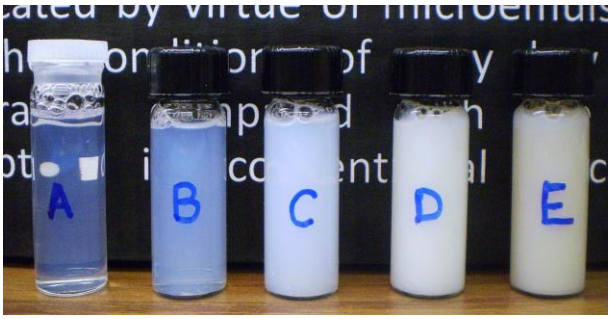

Figure 3. Photographs of obtained latexes: PMMA (A), PMMA/NBR (B), PMMA/PS (C), PMMA/PS/NBR (D), PMMA/PS/HNBR (E). **Polymerization conditions of latex B:** APS = 0.125 g, GS 12-3-12 = 2.0 g, MMA = 3 mL, T = 70 ℃, distilled water = 80 mL at the first stage; AN = 2.5 mL, BD = 7.5 mL, T = 45 ℃ at the second stage. **Polymerization conditions of the rest of latexes**: APS = 0.15 g, Gemini Surfactant 12-3-12 = 2.5 g, MMA = 5 mL, T = 70 ℃, distilled water = 80 mL at the first stage; St = 10 mL, T = 70 ℃ at the second stage; AN = 5 mL, BD = 15 mL, T = 45 ℃ at the third stage.

Figure 3 shows the appearance of PMMA (A), PMMA/NBR (B), PMMA/PS (C), PMMA/PS/NBR (D), PMMA/PS/HNBR (E) nanoparticle latexes. The particle size and solid

content of latexes A, C, and D can be found in Table 1. Latex (B) (PMMA/NBR) was reported previously[29] and is presented here together with the other latexes for comparison purposes. Latex E is the hydrogenated product of Latex D, which has one quarter of the solid content of latex D since a three fold excess of distilled water over the volume of the original latex (v/v) was added during the latex hydrogenation (the experimental method of latex hydrogenation is shown in Supplementary Information). All of the polymer latexes were coagulated using ethanol. It should be noted that GS 12-3-12 is easily dissolved in both ethanol and distilled water. As shown in Figure 3, there is a transition in the appearance of latexes A, C and D varying from transparent to translucent with increasing particle size and solid content. Latex B which is optically transparent, has a number average particle size of 30.6 nm and solid content of 9.7 wt%. Latex E exhibits a reddish-brown color because of the encapsulation of catalyst $RhCl(P(C_6H_5)_3)_3$ within the polymer nanoparticles. $RhCl(P(C_6H_5)_3)_3$ is a red colored solid at room temperature. These colloidal dispersions are stable and can remain suspended in water without precipitation for more than one year at around 6 ℃ inside a refrigerator. This shows that the GS 12-3-12 emulsified semibatch polymerization is an efficient method for synthesizing a stable nanoparticle latex. The zeta potential distribution of PMMA/PS/NBR nanoparticles is provided in Figure S2 in the Supplementary Information. The ζ-potential is +46.1 mV at pH = 3.5 at 25 ℃, which is in good agreement with the observed colloidal stability of the produced latex. pH = 3.5 is the pH value of the obtained latex since the GS 12-3-12 is an acidic salt (quaternary ammonium bromide) in the aqueous phase. In the present polymerization using a cationic surfactant and $(NH_4)_2S_2O_8$ (APS) as the anionic initiator, a net higher positive ζ-potential of particles was still measured. This is due to the relatively higher amount of cationic surfactant than that of APS thereby generating a stronger neutralization effect on the negative ζ-potentials induced by the anionic initiator.

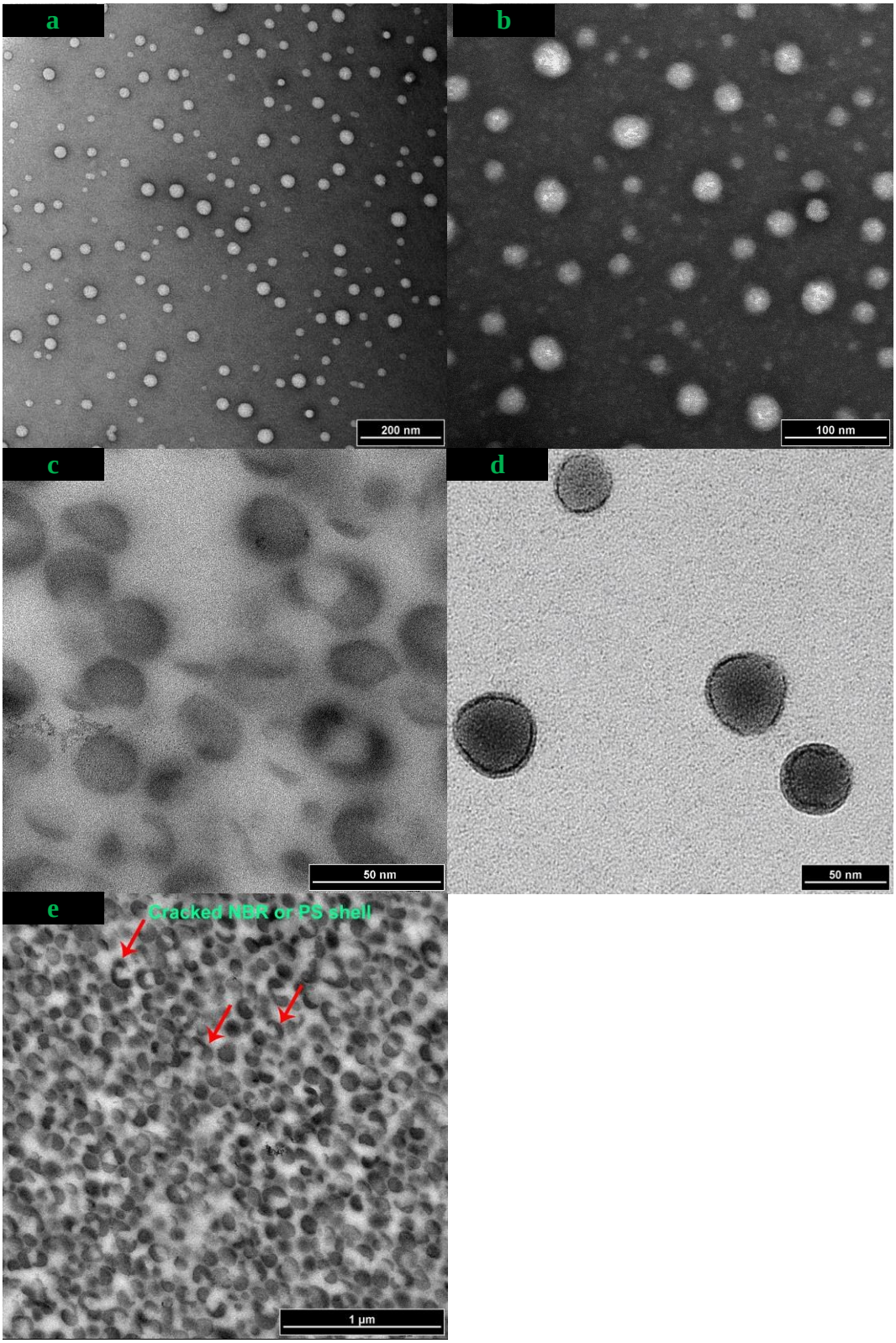

Figure 4. TEM imaging of PMMA, PMMA/PS core-shell and PMMA/PS/NBR tri-layer core-shell nanoparticles after staining with 2% (w/v) uranyl acetate using LEO 912 AB 100kv Energy Filtered TEM. (a), (b), and (d) are the

normal TEM photographs of PMMA, PMMA/PS and PMMA/PS/NBR, respectively. (c) and (e) are the cross-section TEM photographs of PMMA/PS and PMMA/PS/NBR. The sample was carefully ground before sending for the cross-section TEM. **Polymerization conditions**: APS = 0.15 g, Gemini Surfactant 12-3-12 = 2.5 g, MMA = 5 mL, T = 70 ℃, distilled water = 80 mL at the first stage; St = 10 mL, T = 70 ℃ at the second stage; AN = 5 mL, BD = 15 mL, T = 45 ℃ at the third stage.

A set of representative TEM images are presented in Figure 4, which shows the size and morphology of PMMA nanoparticles, PMMA/PS core-shell nanoparticles, and PMMA/PS/NBR trilayer core-shell nanoparticles. As represented by Figures 4a, 4b, and 4d, the obtained PMMA, PMMA/PS, and PMMA/PS/NBR nanoparticles all exhibit a uniform spherical shape. The dimensions of these three types of nanoparticles determined by TEM are consistent with those measured by a DLS technique (Table 1). However, the distinct core-shell structure could not be directly observed from Figure 4b because the contrast between the PMMA domain and PS domain is not sufficiently clear. In general, the PS region is darker than the PMMA region in the TEM observation. Therefore, the coverage of PS layer upon the PMMA polymer weakens the phase contrast between the PMMA and PS phase. The dark background in Figures 4a and 4b is due to the existence of the staining agent uranyl acetate on the copper grid, which increases the contrast between the polymer body (white color in these two figures) and the background. In order to verify the formation of the core-shell structure, cross-sectional TEM was carried out as shown in Figure 4c. It can be seen in Figure 4c that phase separation between the PMMA core and PS shell was observed due to the grinding operation, before sending the samples for analysis by TEM. The PS shell was cracked and bent and the spheres in Figures 4c are the PMMA domains, which further demonstrates that the PMMA/PS nanoparticles obtained have a core-shell nanostructure (the DLS data has provided prima facie evidence as discussed earlier).

In the TEM characterization used in this study, 2% (w/v) uranyl acetate was used to stain the polymer samples. Uranyl acetate is most often used as a negative staining agent, which can enhance the contrast of the sample and the background via a metallic deposit. It is particularly effective for the polymers containing carbon carbon double bonds (C=Cs). As shown in Figure 4d, the overall domains of the PMMA/PS/NBR nanoparticles are quite dark and the background regions are relatively light. This contrast in the color is caused by the binding of uranyl acetate in the C=Cs of the NBR shell. Figure 4d proves that the NBR has been encapsulated upon the PMMA/PS seeded nanoparticles. The PMMA/PS/NBR nanocomposite was also examined by the cross-section TEM as shown in Figure 4e. In this figure, the NBR shell and the PS shell may coexist and it is difficult to distinguish between the NBR or PS shell. However, a conclusion can be drawn from Figure 4e that the NBR shell has been formed in the prepared PMMA/PS/NBR nanoparticles.

The control of the particle morphology is an essential part of semibatch emulsion polymerization. There are many formulation and process factors which can influence or control the morphology and structure composition of the resulting nanoparticles, which are characterized by the type and amount of surfactant and initiator, the manner of monomer feeding, the relatively hydrophilicity of the core and shell monomers, and the interfacial tensions between the polymer-surfactant interface and the polymer-polymer interface.[19,21] The sequential preparation of core and shell particles in multiple stages has been shown here to be an effective approach to obtain complex core-shell structured nanoparticles. The starving induced monomer addition method plays an important role in the formation of a well defined core-shell structure. In this process, the shell monomers have always been at a starving level, which means that the concentration of the shell monomers in the region of each seed is decreased, resulting in that the shell monomers have

no time to diffuse into the inner space of the core polymer and hence are driven to polymerize onto the surface of the core nanoparticles to a greater extent. Meanwhile, due to the lower concentration of monomers within the particles, the internal viscosity of the seeded polymerizing particles becomes high, which thus limits the diffusivity of the shell polymer chains and prevents the shell polymer chains from undergoing Ostwald ripening to form separate spherical microdomains in the core region.

The formation of secondary particles was greatly suppressed in the present polymerization system. During the formation of the core-shell nanostructures, the core monomers are first initiated and then polymerized to form numerous precursors, which are able to provide the nuclei sites for the shell monomers to polymerize on. Therefore, the nucleation energy barrier for the shell polymer which needs to be overcome when no seeds are used, is eliminated, so that the core-shell nanoparticles are formed under kinetic reaction control. The initiation and nucleation of secondary particles is thereby prevented. On the other hand, GS 12-3-12 has a tight packing capability due to their long hydrophobic C_{12} alkyl chains.[36] This constricted packing property results in a cohesive and stable interfacial film around the polymer phase during the polymerization, which enhances the absorption energy between the core polymer domains with surfactant molecules and resists the desorption and repartitioning of the surfactant to stabilize the newly created secondary primary particles.[37]

$RhCl(P(C_6H_5)_3)_3$, is perhaps the most well-known commercially available catalyst for the hydrogenation of unsaturated rubbers. It can achieve complete hydrogenation of the olefin content (C=C) without any reduction of the nitrile group present in NBR. More importantly, it can effectively suppress any crosslinking problems.[32]

Table 2. Direct catalytic latex hydrogenation of PMMA/PS/NBR tri-layer core-shell nanoparticles in the presence of catalyst $RhCl(P(C_6H_5)_3)_3$

Latex label	Blank experiment	PMMA/PS/**HNBR** tri-layer core-shell
Temperature (℃)	130	130
H_2 pressure (psi)	1000	1000
Stirring	Parr stirred reactors	Parr stirred reactors
Turbine type	four-blade impeller	four-blade impeller
Distance from reactor floor (mm)	15	15
Speed (rpm)	600	600
PMMA/PS/NBR latex (mL)	25	25
Added water to above latex (mL)	75	75
Substrate: NBR outer shell (g)	3.4	3.4
Catalyst: $RhCl(P(C_6H_5)_3)_3$ (g)	–	0.034
Ligand: TPP (g)	0.34	0.34
$RhCl(P(C_6H_5)_3)_3$/NBR shell (w/w)	–	1:100
$RhCl(P(C_6H_5)_3)_3$/TPP (w/w)	–	1:10
Reaction time (h)	–	3
Degree of hydrogenation[a]	–	complete hydrogenation
Particle diameter after experiment (nm)[b]	based on DLS data	based on DLS data
D_n	51.8	52.1
D_z	62.9	63.4
PDI of size (D_z/D_n)	1.21	1.22
cross-linking[c]	–	not observed

[a] Determined via ^{1}H NMR analysis (Figure 6).

[b] D_n and D_z were determined by DLS technique and reported as the number average diameter and the intensity average diameter, respectively.

[c] Evaluated via solvent extraction technique.[38]

Table 2 presents the operational conditions and hydrogenation results for the direct catalytic hydrogenation of PMMA/PS/NBR tri-layer core-shell nanoparticles in latex form using $RhCl(P(C_6H_5)_3)_3$. One blank experiment in the absence of catalyst was also listed in Table 2 for the purpose of circumventing the influence of the reactor walls and the agitator in the catalytic reactions. It can be seen from Table 2 that the particle size before and after hydrogenation remained almost unchanged on comparing the original data of particles in Table 1. The TEM imaging of hydrogenated PMMA/PS/NBR is also presented in Figure 5, which confirms that the

produced PMMA/PS/HNBR nanoparticles still maintain the spherical morphology even under the high temperature hydrogenation reactions. In addition, comparing Figure 5 and Figure 4d, it can be seen that the PMMA/PS/HNBR appears brighter and less dark than the PMMA/PS/NBR. This can be explained by the considerable reduction of C=Cs in the HNBR, which results in the less binding of uranyl acetate to the PMMA/PS/HNBR phase.

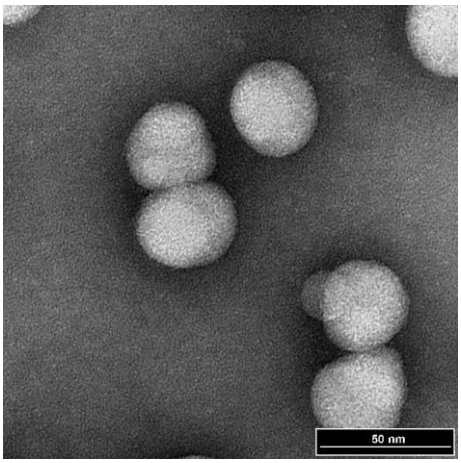

Figure 5. TEM imaging of hydrogenated PMMA/PS/NBR tri-layer core-shell nanoparticles under high-magnification after staining with uranyl acetate using LEO 912 AB 100kv Energy Filtered TEM. **Polymerization conditions**: APS = 0.15 g, Gemini Surfactant 12-3-12 = 2.5 g, MMA = 5 mL, T = 70 ℃, distilled water = 80 mL at the first stage; St = 10 mL, T = 70 ℃ at the second stage; AN = 5 mL, BD = 15 mL, T = 45 ℃ at the third stage. **Hydrogenation conditions**: $RhCl(P(C_6H_5)_3)_3$/NBR shell = 1:100 (w/w), $RhCl(P(C_6H_5)_3)_3$/TPP = 1:10 (w/w), agitation = 600 rpm, T = 130 ℃, P_{H2} = 1000 psi, reaction time = 3 h.

A point worthy of attention here is that the latex hydrogenation reaction presented in this work is a "green" process as it is completely free of organic solvent. Figure 6 shows the ^1H NMR spectra of PMMA/PS/NBR latex nanoparticles for both the pre- and post-hydrogenation reaction catalyzed by $RhCl(P(C_6H_5)_3)_3$ based on the recipe presented in Table 2. The broad doublet in the region of 5.0-5.8 ppm are assigned to the olefinic protons due to the existence of the butadiene unsaturated units. The intensity of the broad doublet in the olefinic region decreased gradually

during the hydrogenation and almost no resonance at all was observed in this range of 5.0-5.8 ppm after 3 h with a $RhCl(P(C_6H_5)_3)_3$/NBR shell weight ratio of 1 wt% at 130 ℃ under 1000 psi (6.89 MPa) of H_2. This result indicated that complete hydrogenation of the NBR layer was obtained. The PMMA/PS/HNBR tri-layer nanoparticles were thereafter achieved as the hydrogenated product. During the hydrogenation operations, no coagulation of the latex was observed, which indicates that this catalytic hydrogenation has no adverse effect on the latex stability. Crosslinking was evaluated via a solvent extraction technique.[38] It was found that no crosslinking occurred in the final hydrogenated product, which demonstrates that the future processibility of the PMMA/PS/HNBR will not be adversely affected by this hydrogenation operation.

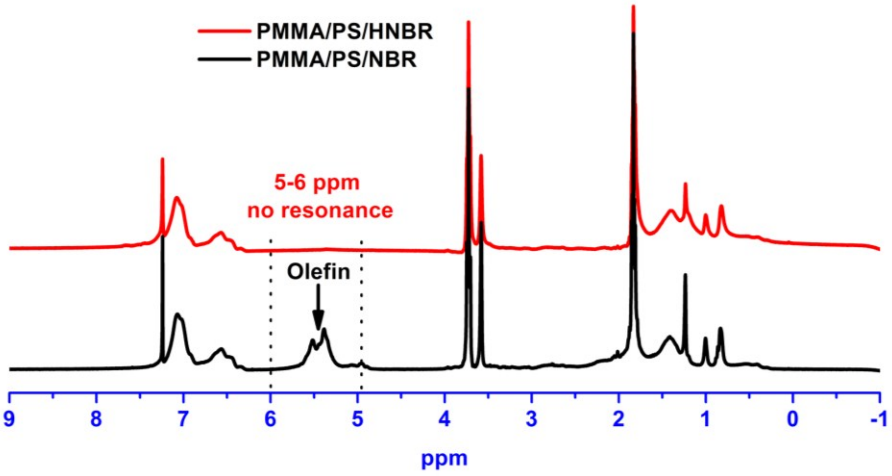

Figure 6. ^{1}HNMR diagram of non-hydrogenation and after hydrogenation of PMMA/PS/NBR nanoparticles. **Polymerization conditions**: APS = 0.15 g, Gemini Surfactant 12-3-12 = 2.5 g, MMA = 5 mL, T = 70 ℃, distilled water = 80 mL at the first stage; St = 10 mL, T = 70 ℃ at the second stage; AN = 5 mL, BD = 15 mL, T = 45 ℃ at the third stage. **Hydrogenation conditions**: $RhCl(P(C_6H_5)_3)_3$/NBR shell = 1:100 (w/w), $RhCl(P(C_6H_5)_3)_3$/TPP = 1:10 (w/w), agitation = 600 rpm, T = 130 ℃, P_{H2} = 1000 psi, reaction time = 3 h.

In our previous report, we studied the direct hydrogenation of ~70 nm commercial NBR latex and 97 mol% conversion was reached after 55 h at a temperature of 145 ℃ under 1000 psi of H_2

pressure with a $RhCl(P(C_6H_5)_3)_3$/NBR weight ratio of 1 wt%.[39] Under the same level of catalyst loading and lower temperature, the hydrogenation of PMMA/PS/NBR nanoparticles shows a significantly faster reaction rate (completed hydrogenation within 3 h with 1 wt% $RhCl(P(C_6H_5)_3)_3$/NBR shell weight ratio at 130 ℃ under 1000 psi of H_2) compared with the commercial ~70 nm NBR nanoparticles. This considerable enhancement in the rate of hydrogenation is due to the fact that nanoparticles (D_n = 51.3 nm, Table 1) with larger specific surface area can increase the capture efficiency for catalyst molecules and the thin layer of less than 20 nm (calculated from the radius difference of PMMA/PS and PMMA/PS/NBR, Table 1) facilitates the diffusion of catalyst molecules inside the NBR chains. The present direct catalytic latex hydrogenation demonstrates that a fast reaction rate can be achieved without using any organic solvent, which may offer exciting avenues in the future for the large-scale production of "green" hydrogenation process.

These core-shell nanoparticles including PMMA/PS, PMMA/PS/NBR, and PMMA/PS/HNBR are expected to play a unique role as performance-enhancing additives and novel reinforcing agents in high performance rubber compounds. They are uniform in spherical shape and have very small particle size with narrow PSD. These nanoparticles provide an opportunity to achieve a more uniform distribution inside the targeted elastomer such as the NBR matrix than in a inorganic filler such as carbon black and silica to meet specific application needs by choosing appropriate core-shell nanoparticles. Given the highly reinforcing nature of these nanoparticles, they can be used as impact modifiers, toughening agents, reinforcing agents, and additives for enhanced performance of the rubber compounds. For example, Wang et al. compared the stress-strain performance between two sulphur vulcanized BR compounds: one reinforced with carbon black and the other with spherical PS/BR nanoparticles with BR as the shell.[22] The results

showed that the BR reinforced with core-shell nanoparticles has a considerably improved modulus at low strains and superior failure properties such as equal tensile strength, higher elongation-to-break, and higher tensile energy-to-break than those using the carbon black as the reinforcing filler. As mentioned above, this is because the polymer nanoparticles have significantly smaller size and are much more easily dispersed in the host rubber than the carbon black fillers, which leads to enhanced compatibility between the host rubber and the reinforcing core of polymer nanoparticles.

Conclusions

We have demonstrated a process-development oriented research which incorporated an emulsion synthesis and green catalysis of a new type of unsaturated polymer nanoparticles. PMMA/PS/NBR tri-layer core-shell diene-based nanoparticles were firstly synthesized by a novel three-stage semibatch emulsion polymerization method. The prepared spherical PMMA/PS/NBR nanoparticles have a very thin NBR layer of less than 20 nm and total *z*-average diameter of 62.5 nm corresponding to a reasonable solid content of 21.7 wt%. The obtained latex is observed to have a good colloidal stability with a ζ-potential of +46.1 mV at pH = 3.5 at 25 ℃. The PMMA/PS/NBR with the NBR outer layer containing 31 wt% nitrile was then used as the substrate for the latex hydrogenation in the presence of Wilkinson's catalyst $RhCl(P(C_6H_5)_3)_3$. A rapid hydrogenation with a complete hydrogenation was obtained within 3 h using 1 wt% $RhCl(P(C_6H_5)_3)_3$/NBR shell at 130 ℃ under 1000 psi of H_2. This latex hydrogenation process was carried out in the absence of any organic solvent and no crosslinking was found in the hydrogenated product, PMMA/PS/HNBR core-shell polymer. This study extended the research on both the synthesis of polymer nanoparticles with complex architecture and chemical modification of high performance elastomers in the aqueous phase. This may

contribute to the development of a "green" process for the commercial hydrogenation of unsaturated rubbers in latex form.

Acknowledgements

The authors thank Mr. Robert Harris (University of Guelph, Canada) for his assistance with the TEM operation. The authors also gratefully acknowledge the support of the Natural Sciences and Engineering Research Council of Canada (NSERC).

References

1 Rao, J. P.; Geckeler, K. E. Prog Polym Sci 2011, 36, 887 887-913.

2 Paul, D. R.; Robeson, L. M. Polymer 2008, 49, 3187-3204.

3 Stuart, M. A. C.; Huck, W. T. S.; Genzer, J.; Müller, M.; Ober, C.; Stamm, M.; Sukhorukov, G. B.; Szleifer, I.; Tsukruk, V.V.; Urban, M.; Winnik, F.; Zauscher, S.; Luzinov, I.; Minko, S. Nat Mater 2010, 9, 101-113.

4 Wen, F.; Zhang, W.; Zheng, P.; Zhang, X.; Yang, X.; Wang, Y.; Jiang, X.; Wei, G.; Shi, L. J Polym Sci Part A: Polym Chem 2008, 46, 1192-1202.

5 Teng, G. H.; Soucek, M. D. J Polym Sci Part A: Polym Chem 2002, 40, 4256-4265.

6 Wooley, K. L. J Polym Sci Part A: Polym Chem 2000, 38, 1397-1407.

7 Si, Q.; Zhou, C.; Yang, H.; Zhang, H. Eur Polym J 2007, 43, 3060-3067.

8 Zhao, J.; Yuan, H.; Pan, Z. J Appl Polym Sci 1994, 53, 1447-1452.

9 Li, C.; Wang, D.; Liu, C. J Disper Sci Technol 2008, 29, 347-350.

10 Wu, S. Polymer 1985, 26, 1855-1863.

11 Wakker, A. Polymer 1991, 32, 279-283.

12 Klapper, M.; Nenov, S.; Haschick, R.; Müller, K.; Müllen, K. Acc Chem Res 2008, 41, 1190-1201.

13 Taylor, J. W.; Winnik, M. A. J Coat Technol Res 2004, 1, 163-190.

14 Schuler, B.; Baumstark, R.; Krisch, S.; Pfau, A.; Sanor, M.; Zosel, A. Prog Org Coat 2000, 40, 139-150.

15 Stubbs, J.; Sundberg, D. J Coat Technol 2003, 75, 59-67.

16 Basset, D. J Coat Technol 2001, 73, 42-55.

17 Lee, C. F. J Polym Sci Part A: Polym Chem 2005, 43, 2224-2236

18 Zhang, M.; Lan, Y.; Wang, D.; Yan, R.; Wang, S.; Yang, L.; Zhang, W. Macromolecules, 2011, 44, 842-847.

19 Liu, W. J.; He, W. D.; Wang, Y. M.; Wang, D.; Zhang, Z. C. Polym Int 2006, 55, 520-524.

20 Ferguson, C. J.; Russell, G. T.; Gilbert, R. G. Polymer 2003, 44, 2607-2619.

21 Tolue, S.; Moghbeli, M. R.; Ghafelebashi, S. M. Eur Polym J 2009, 45, 714-720.

22 Wang, X. R.; Hall, J. E.; Warren, S.; Krom, J.; Magistrelli, J. M.; Rackaitis, M.; Bohm, G. G. A. Macromolecules 2007, 40, 499-508.

23 Garcia, C.; Zhang, Y.; Mahajan, S.; DiSalvo, F.; Wiesner, U. J Am Chem Soc 2003, 125, 13310-13311.

24 Chen, M. Q.; Serizawa, T.; Kishida, A.; Akashi, M. J Polym Sci Part A Polym Chem 1999, 37, 2155-2166.

25 Sanguansap, K.; Suteewong, T.; Saendee, P.; Buranabunya, U.; Tangboriboonrat, P. Polymer 2005, 46, 1373-1378.

26 Li, W. H.; Stover, H. D. H. Macromolecules 2000, 33, 4354-4360.

27 Bai, F.; Yang, X. L.; Huang, W. Q. Macromolecules 2004, 37, 9746–52.

28 Wang, H.; Pan, Q.; Rempel, G. L. J Polym Sci Part A Polym Chem 2012, 50, 4656-4665.

29 Wang, H.; Hammond, M.; Rempel, G. L. J Polym Sci Part A Polym Chem 2012, 50, 736-749.

30 Zana, R.; Benrraou, M.; Rueff, R. Langmuir 1991, 7, 1072-1075

31 Menger, F. M.; Keiper, J. S. Angew Chem Int Ed Engl 2000, 39, 1906-1920.

32 Wang, H.; Yang, L.; Rempel, G. L. Polym Rev 2013, 53, 192-239.

33 Wang, H.; Yang, L.; Scott, S.; Rempel, G. L. J Polym Sci Part A Polym Chem 2012, 50, 4612-4627.

34 Sajjadi, S. Langmuir. 2007, 23, 1018-1024.

35 Full AP, Kaler EW, Arellano J, Puig JE. Macromolecules 1996;29:2764–75.

36 Hait, S. K.; Moulik, S. P. Curr Sci 2002, 82, 1101-1111.

37 Ha, J. W.; Park, I. J.; Lee, S. B.; Kim, D. K. Macromolecules 2002, 35, 6811-6818.

38 (a) He, Y.; Daniels, E. S.; Klein, A.; El-Aasser, M. S. J Appl Polym Sci 1996, 65, 511-523. (b) He, Y.; Daniels, E. S.; Klein, A.; El-Aasser, M. S. J Appl Polym Sci 1997, 64, 1143-1152.

39 Wei, Z.; Wu, J.; Pan, Q.; Rempel, G. L. Macromol Rapid Commun 2005, 26, 1768-1772.

Supplementary Information

for

Preparation of Poly(methyl methacrylate)/Polystyrene/Poly(acrylonitrile-*co*-butadiene) Tri-layer Core-Shell Nanoparticles and Their Postpolymerization Modification via Catalytic Latex Hydrogenation

Hui Wang, Lijuan Yang, Garry L. Rempel*

Department of Chemical Engineering, University of Waterloo, 200 University Ave. West, Waterloo, Ontario, N2L 3G1, Canada

Author information

Hui Wang, h54wang@uwaterloo.ca;

Lijuan Yang, l32yang@uwaterloo.ca;

*Corresponding author: Garry L. Rempel, grempel@uwaterloo.ca; Tel.: +1 519 8884567 ext. 32702. Fax: +1 519 7464979.

Table of contents	**Pages**
1. Experimental Section	S2-S4
2. Characterization	S5-S7
3. Figure	S8-S9
4. Reference	S9-S10

Experimental Section

Materials Used in Synthesis of Polymer Nanoparticles

Ammonium persulfate (APS, 98%), methyl methacrylate (MMA, 99%), acrylonitrile (AN, 99+%) and styrene (St, 99%) were purchased from Aldrich. The inhibitors were removed prior to polymerization by passing the monomer AN through an alumina column. The initiator APS was purified by recrystallization in ethanol and dried under vacuum at room temperature. The 1,3-Butadiene (BD) was provided by LANXESS Inc. The Gemini surfactant 12-3-12, i.e., trimethylene-1,3-bis(dodecyldimethylammonium bromide) with molar mass = 628.69 g/mol was synthesized by known procedures[1] and used after repeated recrystallization from acetone-ethyl acetate (1:1 volume). The ethanol, methanol, acetone, and ethyl acetate were all reagent grade and used without further purification. These four organic solvents and distilled water were obtained from the Department of Chemical Engineering, University of Waterloo, Canada.

Materials for Direct Hydrogenation in Latex Form

Ultra-high purity hydrogen (99.999%, oxygen-free) was used as received (Praxair Inc. Mississauga, CA). Wilkinson's catalyst $RhCl(P(C_6H_5)_3)_3$ was prepared according to the literature.[2,3] Triphenylphosphine (TPP, 99%) was obtained from Strem Chemicals, Inc. (Massachusetts, US) and further purified by recrystallization from ethanol to remove triphenylphosphine oxide.

Synthesis of PMMA/PS/NBR Nanoparticles

The PMMA/PS/NBR tri-layer core-shell nanoparticles were prepared via a multistage semibatch emulsion polymerization, which was performed in a Parr 316 Stainless Steel Parr reactor (**Figure S1**). In the first stage of the preparation of PMMA seeded latex, 2.5

g of GS 12-3-12, 0.15 g APS, and 80 mL distilled water were charged into the stainless steel reactor equipped with an impeller stirrer, an addition tube, and a thermocouple. Oxygen was removed by purging a slow stream of nitrogen gas for 20 min while stirring was maintained at 200 rpm. The reactor was then heated up to the reaction temperature for the first stage at 70 ℃. The monomer MMA (5 mL) was fed continuously to the reactor using a designed addition tube at a constant rate of 0.05 mL/min. After the MMA feeding was completed, the reaction system was allowed to proceed for an additional 1 h. Under the same temperature, the second monomer styrene (10 mL) was then fed in the reactor in an identical manner and with the same rate of addition as the MMA to prepare the PMMA/PS core-shell nanoparticles during this second stage of polymerization. After the completion of the addition of styrene, the temperature was decreased from 70 to 45 ℃ as the copolymerization temperature of AN and BD for the shell formation was set at 45 ℃. The reaction system was aged for 1 h before proceeding to the third stage copolymerization of AN and BD. In the third stage, it is important to increase the pressure inside the reactor to at least 22 psi using nitrogen gas (80 psi used in our studies), since the saturated vapor pressure of BD in the addition tube is around 22 psi at room temperature. The addition tube filled with a 5 mL AN/15 mL BD mixture was then connected with the reactor (80 psi) and the pressure between the reactor and the addition tube was thereafter balanced. The mixture of AN and BD was added continuously at the same rate of 0.05 mL/min. After the completion of the addition, the polymerization was aged for a given time to reach a reasonable conversion.

Direct Hydrogenation of PMMA/PS/NBR Core-Shell Nanosized Latex

The latex hydrogenation of diene-based nanoparticles in the presence of Wilkinson's catalyst $RhCl(P(C_6H_5)_3)_3$ was carried out in the same Parr reactor as the polymerization for the synthesis of nanoparticle substrate (**Figure S1**). A measured volume of the latex (25 mL) with the added distilled water (75 mL) were first mixed with 1 wt% $RhCl(P(C_6H_5)_3)_3$ on the basis of the amount of the NBR layer and the additive TPP with a weight ratio of 10:1 to catalyst. The TPP plays a vital role in the hydrogenation reaction as it maintains the activity of Wilkinson's catalyst.[4] The mixture was then degassed with three quick N_2 cycles and subjected to bubbling N_2 under about 1.38 MPa for 20 min at room temperature with an agitation speed of 200 rpm. The resulting mixture was heated up to 130 ℃ and stabilized for 2 h under 600 rpm stirring speed. The hydrogenation reaction was embarked on when hydrogen gas at a pressure of 6.89 MPa was introduced into the reactor. The hydrogen pressure (6.89 MPa), hydrogenation temperature (130 ℃), and agitation speed (600 rpm) were maintained constant throughout the reaction period. Aliquots were taken at various time intervals through a dip tube for the characterization. After a given reaction time, the system was cooled down to room temperature and depressurized to obtain the final product.

Characterization Section

Method to Obtain the Polymer Solid

The polymer latexes were coagulated in ethanol. It is noted that GS 12-3-12 is easily dissolved in both ethanol and distilled water. The filtered solid was dried under vacuum in an oven at room temperature until constant weight was reached. The polymerization conversions of monomer(s) were calculated by a gravimetric method.

Proton Nuclear Magnetic Resonance (^{1}H NMR)

The ^{1}H NMR was also performed to investigate the composition and microstructure of the polymer NPs. The ^{1}H NMR spectra were recorded on a Bruker 300 MHz Spectrometer (Bruker BioSpin Corp. Massachusetts, US) and chemical shifts were reported in ppm units with TMS as an internal standard. The sample solution was prepared by dissolving 15-20 mg dried polymer solid into 1 mL $CDCl_3$.

Dynamic Light Scattering

The size and number size distribution (non-negative least squares method) of the polymer particles of the synthesized latex were determined by dynamic light scattering (DLS) at 25 ℃ using a Nanotrac 150 particle size analyzer (BETATEK Inc., Canada) and reported as the number average diameter. The calculations of the particle size distributions were performed using Microtrac FLEX 10.2.14 software available from BETATEK Inc., which employed single-exponential fitting, non-negatively constrained least-squares (NNLS), cumulants analysis, and CONTIN particle size distribution analysis routines.

Transmission Electron Microscopy

LEO 912 AB 100 kV Energy Filtered Transmission Electron Microscopy (EFTEM) (Carl Zeiss Inc. Germany) was used to examine the size and observe the morphology of the

nanoparticles. When preparing the specimens for TEM measurement, the nanosized latex was first diluted with distilled water and then 10 μL of the diluted solution was incubated on a 400-mesh copper grid at room temperature. Excess solution was drawn off the edge of the grid with tissue paper. Next the grid was negatively stained with 2% (w/v) uranyl acetate for 1 min. After the excess stains were drawn off with tissue paper, the grid was delivered into the TEM chamber for imaging.

Cross Section TEM

Before sending the samples for the analysis of cross section TEM, the samples were first carefully ground and then immersed in 100% ethanol for 2 hr with three changes of ethanol. The ethanol was then removed and replaced with a 50/50 (v/v) mixture of ethanol and LR White resin. This was left overnight with mixing. The 50/50 mixture was replaced by pure LR White resin and stirred for 3 hr. The sample was then put into a gelatin capsule. Once the sample had sunk to the bottom of the capsule the resin was polymerized at 60 ℃ overnight. Thin sections around 75 nm thick were cut with an ultramicrotome. The resulting sections were mounted on 100-mesh copper grids and stained with 2% (w/v) uranyl acetate (7 min) and Reynold's lead citrate (3 min). The prepared samples were viewed using a LEO 912 AB EFTEM.

Cross-linking Examination

The cross-linking was estimated using a solvent extraction technique, which has been in detail described in El-Aasser and coworkers' reports.[5,6]

Zeta-potential

The ζ-potential measurements of core and core-shell latex particles were determined using a Zetasizer Nano ZS (Malvern Instruments, Worcestershire, UK) at 25 ℃. The

latex samples were injected into a disposable cell (folded capillary DTS-1060 from Malvern, Worcestershire, UK) with a volume of ~1 mL and analyzed at constant voltage. The ζ-potential distribution (in mV) was automatically calculated from the electrophoretic mobility distribution based on the Smoluchowski formula. For each sample, the ζ-potential measurement was repeated three times and the mean value was reported. The ζ-potentials reported herein correspond to the average of the peak values of the ζ-potential distributions.

Molecular Weight

The molecular weight and polydispersity index were determined by size exclusion chromatography (SEC, Model 305 TDA, Viscotek, Houston, US). The dried polymers were first dissolved in THF and filtered through a 25 mm syringe filter with a 450 nm GHP membrane (Pall Corp. New York, US) and then 100 μL of the solution was injected into the SEC analysis column using THF (GPC grade, stabilized with 250 ppm of 2,6-Di-tert-butyl-4-methylphenol (BHT)) as the eluent at a flow rate of 1.0 mL/min at 25 ℃. The detectors are a triple detector system with a multi-angled laser light scattering setup equipped with an RI detector and a Viscometer detector. Polystyrene standard (PS 99 K, $\overline{M}_w$ = 98251, $\overline{M}_n$ = 96722, IV = 0.477 in THF at 30 ℃) was used for calibration.

Figure Section

The synthesis and hydrogenation of nanoparticles was performed in a modified Parr 316 Stainless Steel reactor (**Figure S1**).

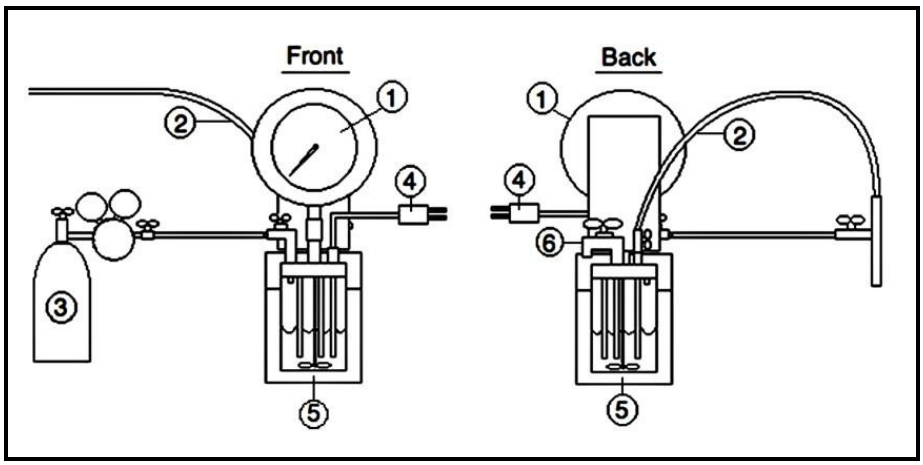

Figure S1. Modified Parr 316 Stainless Steel Reactor. ① pressure gauge; ② monomer adding tube for polymerization of monomers or the hydrogen feeding for the hydrogenation reaction; ③ nitrogen cylinder; ④ thermocouple; ⑤ reactor autoclave; ⑥ sample taken outlet tube.

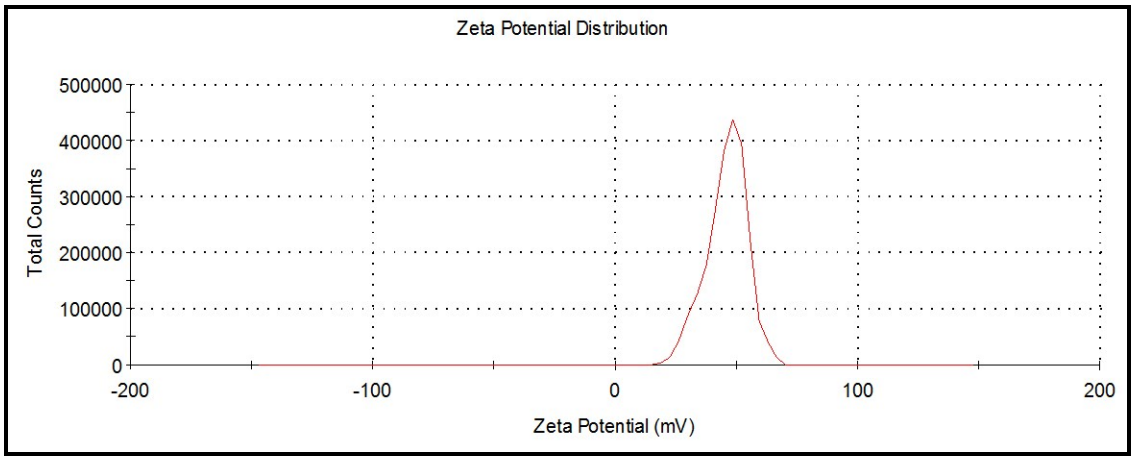

Figure S2. Zeta potential distribution oof PMMA/PS/NBR latex nanoparticles. **Experimental conditions of synthesis of PMMA/PS/NBR nanosize latex**: APS = 0.15 g, Gemini Surfactant 12-3-12 = 2.5 g, MMA = 5.0 mL, T = 70 ℃ at the first stage; Styrene = 10 mL, T = 70 ℃ at the second stage; AN = 2.5 mL, BD = 7.5 mL, T = 45 ℃ at the third stage.

The average ζ-potential was reported to be 46.1 mV at pH = 3.5 at 25 ℃, which represents a good stability of the obtained latex.

References

1 Zana, R.; Benrraou, M.; Rueff, R. Langmuir 1991, 7, 1072-1075.

2 Osborn, J. A.; Jardine, F. H.; Young, J. F.; Wilkinson, G. J. Chem. Soc. A. 1966, 12, 1711–1732.

3 Parent, J. S.; McManus, N. T.; Rempel, G. L. Ind. Eng. Chem. Res. 1996, 35, 4417–4423.

4 Wang H, Yang L, Scott S, Rempel GL (2012) J Polym Sci Part A Polym Chem 50(22):4612.

5 He, Y.; Daniels, E. S.; Klein, A.; El-Aasser, M. S. J Appl Polym Sci 1996, 65, 511-523.

6 He, Y.; Daniels, E. S.; Klein, A.; El-Aasser, M. S. J Appl Polym Sci 1997, 64, 1143-1152.